Biomass and Bioenergy 166 (2022) 106623

Contents lists available at ScienceDirect

Biomass and Bioenergy

journal homepage: www.elsevier.com/locate/biombioe

Recovery of oils and antioxidants from olive stones

Joseph B.D. Osei [a], Amirpiran Amiri [a], Jiawei Wang [a], Marcia T. Tavares [b], Worapon Kiatkittipong [c], Vesna Najdanovic-Visak [a,*]

[a] Chemical Engineering and Applied Chemistry, Energy & Bioproducts Research Institute, Aston University, Birmingham B4 7ET, United Kingdom
[b] LAQV-REQUIMTE, Departamento de Química, Faculdade de Ciências e Tecnologia, Universidade NOVA de Lisboa, Caparica, 2829-516, Portugal
[c] Department of Chemical Engineering, Faculty of Engineering and Industrial Technology, Silpakorn University, Nakhon Pathom, 73000, Thailand

ARTICLE INFO

Keywords:
Olive stones
Antioxidants
Kinetics of oil extraction
Thermodynamics of oil extraction
Gastrointestinal digestion
Solvent extraction

ABSTRACT

The olive oil industry generates enormous amounts of olive stones each year, which have the potential to be used as a biofuel but have high oil content, which negatively impacts the combustion process. In addition, olive stones contain high-value antioxidants, and their exploitation can provide additional revenues for the biofuel industry.

In this work, we report the effect of different extraction solvents on the extraction of antioxidants and their activity. In addition, in vitro gastrointestinal digestion was used to evaluate the content and antioxidant activity of the olive stone extracts after gastrointestinal digestion. The extracts obtained by aqueous ethanol solvent (50% vol) exhibited the highest antioxidant activity with the *DPPH* IC50 of 1.27 mg mL^{-1} and ferric reducing antioxidant power (*FRAP*) of 6.33 mg AAE g^{-1}. After in vitro digestion composed of gastric and intestinal processes, the antioxidant activity of olive stones decreased: *DPPH* IC50 value increased three times (a higher value of IC50 indicates lower antioxidant activity) and *FRAP* decreased almost five times with respect to the values obtained for original extracts.

Furthermore, both phenomenological and shrinking core models were used to fit experimental oil extraction kinetics data and showed good agreement. Thermodynamic analysis showed that the extraction process is endothermic and irreversible while spontaneous and thermodynamically favourable for all conditions except for oil extraction from olive stones of 3.10 mm particle size at 20 °C. The calculated value for temperature coefficient is in good agreement with the previously reported values for the oil extraction from similar biomass.

1. Introduction

In the last decade, various worldwide initiatives have been developed to promote the utilization of waste streams, increase resource efficiency and reduce environmental impacts. Examples include the United Nations, the World Economic Forum and the European Union, all advocating a transition to a more circular economic model, where the waste is used as resources to produce valuable chemicals.

Enormous amounts of agri-food waste are produced yearly and are rich in proteins, carbohydrates, and various bioactive compounds [1]. Therefore, processing food waste can get additional revenues and reduce waste and associated landfills [2]. Olive stones, a by-product of the olive oil production process, are an example of agricultural food waste that can be used as a raw material to produce fuels and chemicals. Approximately 4 million tonnes of olive stone are generated globally, mainly in Mediterranean countries [3]. This lignocellulosic material, composed mainly of hemicellulose, cellulose and lignin, has a net calorific value of approximately 18 MJ kg^{-1} [4], making it an excellent candidate to be used as a solid biofuel for heating and generating electrical and thermal energy. Unlike other solid biofuels such as firewood and wooden briquettes, chips and pellets, olive stones contain oils, which negatively impact the combustion process. In combustion tests in boilers and stoves, oil contents above 1% increased carbon monoxide emissions, nitrogen oxides, organic carbon, solid particles, and particulate matter PM1 and PM0.1 [5]. Therefore, studying prior oil removal is of utmost importance for assessing the production rate, energy consumption, process minimization and ultimately determining the industrial applicability. Chanioti et al. [6] studied oil extraction kinetics from olive pomace containing olive skin, pulp, stone and kernel under different process conditions, but the oil extraction kinetics from olive stones is solely unknown.

Olive stones are also a rich source of proteins, oils, fibres,

* Corresponding author.
E-mail address: v.najdanovic@aston.ac.uk (V. Najdanovic-Visak).

https://doi.org/10.1016/j.biombioe.2022.106623
Received 30 June 2022; Received in revised form 19 September 2022; Accepted 9 October 2022
Available online 21 October 2022

antioxidants and other compounds, which can be recovered and utilized as food additives, nutraceuticals, pharmaceuticals and cosmeceuticals [7]. The phenolic profile of olive stones revealed the presence of tyrosol, hydroxytyrosol, oleuropein and oleuropein-aglycone di-aldehyde (3, 4-DHPEA-EDA) [8]. These compounds are known to have various biological effects, such as antiatherogenic, cardioprotective, anticancer, neuroprotective, antidiabetic and antiobesity [9]. Therefore, this agricultural waste could be exploited to produce valuable chemicals, providing additional revenues for the biofuel industry and enhancing its competitiveness on a global scale. Another drive comes from the consumers' demands to substitute currently used synthetic food antioxidants with naturally derived, additive-free and safe products.

Lama-Munoz et al. [10] have proposed a two-step process: to recover antioxidants from olive stones in the first step, followed by producing fermentable sugars. The authors studied the influence of temperature, time, and sulphuric acid concentration in water. Concerning the antioxidant activity of obtained extracts, the best result was obtained at 130 °C and after 90 min. In another study [11], hot ethanol was also proposed as a solvent for extracting antioxidants from previously defatted olive stones, concluding that obtained extracts could be suitable for various applications.

Not all of the antioxidant compounds present in biomass extracts can be absorbed by the human body because of the different physicochemical and biochemical conditions during digestion. Furthermore, their antioxidant activity depends on the amount consumed and their bioavailability which is influenced by surrounding pH, temperature, oxygen content, light intensity, enzyme activity, solubility as well as interaction with other dietary ingredients released during digestion [12]. Once consumed and going through the digestive system, these compounds may undergo changes that modify their beneficial effects. Thus, it is essential to determine the influence of the digestion process on the chemical stability of the obtained extracts. To this end, various in vitro digestion models have been widely used, as recently reviewed by Wojtunik-Kulesza et al. [13]. Most models are static gastrointestinal models, which simulate transit through the human digestive tract by sequential exposure of the extract to simulated mouth, gastric, and small intestinal conditions and consequent monitoring of their antioxidant activities [14].

The objectives of this study were to: (1) study the influence of using different extraction solvents on the antioxidant content (phenolic, flavonoid and tannin) and antioxidant activity of obtained extracts; (2) establish the kinetics of oil extraction from olive stones using n-hexane by both experimental determinations and modelling; (3) evaluate the content and antioxidant activity of the olive stone extracts after in vitro gastrointestinal digestion.

2. Methods

2.1. Chemicals and materials

All chemicals used in this study were purchased from Sigma Aldrich and were used without further treatment. Their names, molecular formulas, CAS numbers and stated purity are shown in Table S1 (Supplementary Information).

Crushed and air-dried olive stones were supplied from Griffin Renewables ltd. A lab grinder (IKA M 20 Universal mill) was used to reduce olive stone particle size follower by sieve structure composed of four sieve openings, 3.35, 2.80, 1.18 and 1.00 mm. Two sieve fractions were used with particle size ranges of 2.8–3.35 mm and 1.00–1.18 mm. Their average particle diameter of 3.10 mm and 1.04 mm were determined by a laser diffraction analyzer (Malvern Mastersizer model 3000).

2.2. Extraction of antioxidants

The extraction of the antioxidants from the olive stones (particle size 1.04 mm) was studied using a 500 mL round-bottom flask with a magnetic stirrer and fitted condenser to avoid solvent losses. Olive stones (7.50 g) were mixed with 150 mL of solvent in the flask. The flask was immersed in a water bath controlled by a temperature controller (Stuart, model WZ-04805-92). The temperature of the extraction process was 25 °C. Different solvents were tested for the extraction of antioxidants, including acetone, ethanol, methanol and water, as well as their aqueous solutions (50% vol).

The mixtures were filtered using a Büchner funnel. Extracted solids were discarded while obtained supernatants were dried using a rotary evaporator (BUCHI Rotavapor R-300) at 45 °C to obtain dry extracts that were subsequently kept, in the dark, in the refrigerator before further analysis. The extraction yield was calculated as the ratio of the mass of the obtained extract to the mass of the dry weight of olive stones.

Obtained dry extracts were diluted before analysis to determine antioxidant content (total phenolic and condensed tannin contents) and antioxidant activities (*DPPH* and ferric reducing antioxidant power).

2.3. Antioxidant content

2.3.1. Total phenolic content

The method of Kahkonen et al. [15] was used to determine the total phenolic content in the extracts. A volume of 0.2 mL of the extract solution (10 mg mL^{-1}) was mixed with 1 mL of Folin Ciocalteu reagent and 0.8 mL of 7.5% (mass per volume) sodium carbonate. The resulting solution was incubated at room temperature for 60 min in the dark. Subsequently, the absorbance was measured at 740 nm using UV–Visible Spectrophotometer (Evolution 220, Thermo Fisher Scientific). The results are represented as mg of gallic acid equivalents per g of dry olive stones (mgGAE g^{-1}) by means of calibration curves with standard gallic acid solutions.

2.3.2. Condensed tannins content

The condensed tannins content of the extracts was determined using a method developed by Swain and Hillis [16]. One mL of the extract solution (5 mg mL^{-1}) was mixed with 2 mL of vanillin solution (1% mass per volume in 70% vol of sulphuric acid). The resulting solution was incubated at 50 °C for 20 min, and subsequently, the absorbance was measured at 500 nm using UV–Vis Spectrophotometer (Evolution 220, Thermo Fisher Scientific). Results are expressed as mg of catechin equivalents per g of dry olive stones (mg CE g^{-1}) by means of calibration curves with standard catechin solutions.

2.4. Antioxidant activity

2.4.1. DPPH assay

The free radical-scavenging activity of the extracts was determined according to the method described by Kroyer and Hegedus [17] using the stable radical DPPH• (1,1-diphenyl-2-picrylhydrazyl). A volume of 0.3 mL of the extract solution was added to 2.7 mL of 60 μM DPPH solution and the resulting solution was incubated at room temperature for 60 min in the dark. The absorbance was measured at 517 nm using UV–Visible Spectrophotometer (Evolution 220, Thermo Fisher Scientific). The percentage of DPPH• radical scavenging activity of each extract was calculated according to the following equation:

$$\%DPPH\ inhibition = \frac{A_c - A_s}{Ac} \quad (1)$$

where A_c and A_s are the absorbances of the control and extract solutions, respectively. The absorption decrease at 517 nm was used to calculate the IC50 (mg mL^{-1}). Ascorbic acid was used as a standard.

2.4.2. Ferric reducing antioxidant power assay

The ferric reducing antioxidant power (*FRAP*) was determined according to the method described by Yildirim et al. [18]. A volume of 1 mL of the extract solution was mixed with 2.5 mL of phosphate buffer

(0.2 M, pH 6.6) and 2.5 mL of potassium ferricyanide (1% mass per volume). After 20 min of incubation at 50 °C, 2.5 mL of trichloroacetic acid (10% mass per volume) was added and mixed well. A volume of 1.25 mL of the resulting mixture was mixed with 1.25 mL of distilled water and 0.25 mL of aqueous ferric chloride solution (0.1% mass per volume). The absorbance was measured at 700 nm after 10 min. The ferric reducing power was expressed as mg ascorbic acid per g of dry olive stones (mg AAE g^{-1}).

2.4.3. In vitro digestion of antioxidants

The extracts were submitted to an in vitro gastric and intestinal digestions following methods previously published [19,20] with some modifications. For the gastric digestion, an initial solution of 50 mL NaCl (0.9%), 8 mL HCl (0.1 M) and 4 mL pepsin solution (40 mg mL^{-1} in 0.1 M HCl) was mixed with 6.4 mL of extract (50 mg mL^{-1}) and the pH was then adjusted (2–2.5). The resulting gastric solution was incubated for 1 h in a shaking water bath at 37 °C, and aliquots were stored at −20 °C until further analysis.

For intestinal digestion, the gastric solution was neutralized to a target pH of 6.5 using 0.1 M $NaHCO_3$ and then added 18 mL of pancreatin-bile extract mixture (2 mg mL^{-1} pancreatin and 12 mg mL^{-1} bile extract dissolved in 0.1 M $NaHCO_3$). The mixture was further incubated for 2 h in a shaking water bath at 37 °C. The pH was then measured at 7–7.5 and aliquots were stored at −20 °C until further analysis of total phenolic and condensed tannins contents as well as their antioxidant activity (*DPPH* and *FRAP*) described in the above sections.

2.4.4. Data and statistical analysis

All the measurements of total phenolic and condensed tannin contents as well as antioxidant activities (*DPPH* and *FRAP*) of the olive stones extracts were conducted in triplicate. All results are presented as mean ± standard deviation.

2.5. Oil extraction

2.5.1. Soxhlet extraction

Initially, the oil content of the dried olive stones was determined using a Soxhlet extractor with n-hexane as a solvent. Before commencing the work, the time taken to obtain the maximum amount of oils was estimated by performing the Soxhlet extraction at different time intervals, and it was determined that 6 h was sufficient. A known amount of olive stones (approximately 30 g) was used and the extraction was carried out for 6 h at 69 °C. Subsequently, the obtained mixture of n-hexane with extracted oils was placed in a rotary evaporator to evaporate h-hexane. The amount of the extracted oil was determined gravimetrically using the analytical balance. The oil content is expressed as a percentage mass of extracted oil with respect to the dry mass of olive stones.

2.5.2. Kinetics of oil extraction

Kinetics of oil extraction from olive stones using n-hexane as a solvent was performed in a batch extractor system composed of a 1-L round-bottom flask with a three-necked top. The flask is equipped with a magnetic stirrer and a condenser to avoid solvents losses. The flask was immersed in a water bath controlled by a temperature controller (Stuart, model WZ-04805-92). A volume of 375 mL of n-hexane was first heated to the wanted temperature (20 °C, 30 °C, 40 °C or 60 °C), and only then 25 g of olive stones were added (solid-to-solvent ratio of 15 mL g^{-1}). Two different particle sizes of olive stones (3.10 mm and 1.04 mm) were tested.

The extraction mixture samples (1 mL) were taken at regular intervals and placed in pre-weighed vials. Subsequently, the solvent was evaporated and the amount of oil extracted in each time interval was determined by measuring the mass of the residue. Extractions were repeated at least three times for each of the experimental conditions. Extraction yield at time t (Y_t) was calculated as:

$$Y_t(\%) = \frac{\text{mass of oil extracted at time } t}{\text{mass of dry olive stones}} \bullet 100 \quad (2)$$

The average deviation of the extraction yield Y_t was ±0.2%.

Extraction yields were measured after 30 min, 1 h, 2 h and 3 h in order to estimate the time needed to reach saturation. It was concluded that 1 h is sufficient time to reach saturation.

2.5.3. Kinetics of oil extraction modelling

The phenomenological model described in detail by Kostic et al. [21] and previously used by So and McDonald [22] was used to model the oil extraction:

$$Y_t = Y_\infty \left[1 - f \bullet e^{-k_w \bullet t} - (1-f) e^{-k_d \bullet t}\right] \quad (3)$$

where f and $(1 - f)$ represent the fractions of oil extracted from olive stones into the solution by washing and diffusion, k_w and k_d are rate constants (volumetric mass transfer coefficients) of washing and diffusion, respectively, while Y_t and Y_∞ stand for oil extraction yield at time t and at saturation, respectively.

The model is based on a number of assumptions:

- solid and solvent are mixed in a batch extractor until reaching saturation;
- there is no mass transfer limitation in the bulk of the liquid phase;
- oil extracted from olive stones is a pseudo-single component;
- solid particles are pseudo particles of average initial oil content and size;
- two simultaneous mechanisms occur, washing and diffusion;
- both mass transfer coefficients of both washing and diffusion are constant;
- total oil concentration with time is a sum of oil concentrations resulting from washing and diffusion.

Kinetics of oil extraction data were fitted to equation (3) and fitting parameters (Y_∞, f, k_w and k_d) were obtained by regression.

To compare the experimental data and data predicted by both models, root mean square deviation (*RMSD*) and coefficient of determination (r^2) were used according to Equations (4) and (5):

$$RMSD = \sqrt{\frac{\sum_i \left(Y_t^{calc} - Y_t^{exp}\right)^2}{N}} \quad (4)$$

$$r^2 = 1 - \frac{\sum_i \left(Y_t^{exp} - Y_t^{calc}\right)^2}{\sum_i \left(Y_t^{exp} - Y_t^{mean}\right)^2} \quad (5)$$

where Y_t^{exp}, Y_t^{calc} and Y_t^{mean} are the experimental, calculated and mean values of the oil yield, respectively, whilst N stands for the number of data points.

2.5.4. Shrinking core model

The extraction of oil or other compounds from plant biomass can be estimated based on first-principle mass and heat transfer rates linked with an expression of pseudo intrinsic extraction kinetics. To this end, understanding of the dominant controlling mechanism(s) is key to set up the governing and constitutive equations in a predictive model. The shrinking core model (SCM), developed by Yagi and Kunii [23,24], has been effectively applied to many gas-solid and liquid-solid reactive cases where mass transfer, heat transfer and reaction kinetics are interplaying factors in the process [25,26]. By establishing an analogy between reaction and extraction kinetics, the SCM was deployed in this study to capture the real-time changes of the particles.

The schematic of the solid particle model is shown in Fig. 1. The model accounts for three contributions: diffusion through liquid film

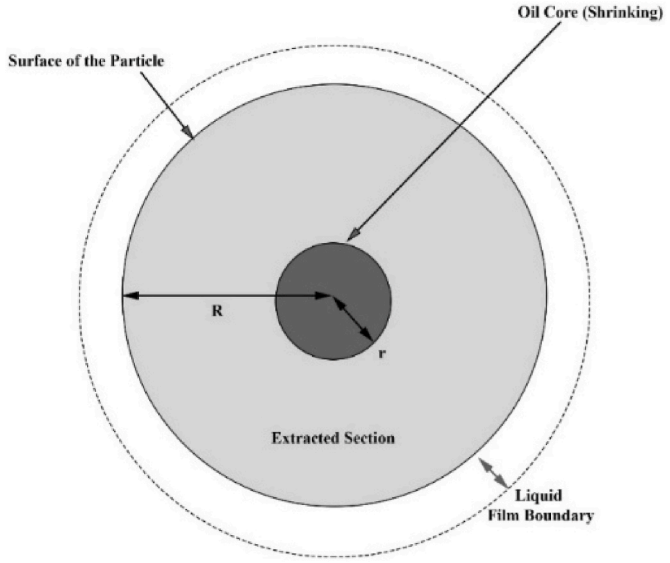

Fig. 1. Schematic diagram of the Shrinking Core Model (SCM) assuming the olive stone particle as a sphere.

surrounding the particle, a depleted solid layer (called ash layer) and intrinsic extraction rate (the oil extraction rate when no heat or mass transfer resistance exists). The ash layer (the extracted section) was considered the seed's vegetal (cell) structure from which oil is fully extracted.

In developing a variation of SCM for this case study, the following assumptions were made:

- Solute (oil) extracted from olive stones is a pseudo-single component;
- Oil is homogeneously distributed within the seed particle;
- The extraction process is isobaric and isothermal;
- The oil concentration at the particle surface is approximately constant and equal to bulk concentration;
- The size of the particle is not changed during the extraction process;
- The role of liquid film surrounding the particle in controlling the extraction rate is negligible. This is shown when the model is compared against the experimental data.

When the rate of solvent diffusion in extracted (ash) layer is slow enough to be considered the main controlling factor, the extraction time will be a strong function of the mass transfer rate term and other mechanisms involved can be ignored in the model. This is called a diffusion-controlled system that will result in a diffusion-control model (DCM). In the DCM, the extraction time as a function of extraction yield is given by equation (6):

$$\frac{t}{\tau} = 1 - 3(1 - X_{oil})^{2/3} + 2(1 - X_{oil}) \tag{6}$$

where t, τ, X stand for a time, full extraction time, and extraction yield, respectively. If DCM applies, the best fitting can be achieved based on τ tuning (a group number that consists of the particle size, diffusivity and surrounding concentration). When DCM applies, the best τ searched through an optimization process can be used to approximate the diffusivity numerically.

When the diffusion rate in the extracted layer is very high compared to the inherent extraction rate, the presence of the 'ash layer' does not considerably influence the extraction progress. In such a case, the time is mainly controlled by the inherent extraction term, while other rates can be ignored. This results in a so-called extraction-control model (ECM). The ECM estimates the overall extraction rate through equation (7):

$$\frac{t}{\tau} = 1 - \frac{r_c}{R} = 1 - (1 - X_{oil})^{1/3} \tag{7}$$

The fitting parameter is τ which includes the extraction rate coefficient. When ECM applies to the extraction system and the extraction driving force is known, the best τ values can be used to approximate the extraction rate coefficient numerically.

A linear relationship between the oil yield and extraction time is expected when the liquid film (surrounding the particle) dominates the overall rate. In this work, experiments were carried out in a well-mixed system reducing external mass transfer resistance, and therefore, it was assumed that the role of the surrounding liquid is negligible.

2.5.4. Thermodynamic properties of oil extraction

The enthalpy change (ΔH^0) and entropy change (ΔS^0) were determined using the van't Hoff equation:

$$\ln K = -\frac{\Delta H^0}{RT} + \frac{\Delta S^0}{R} \tag{8}$$

where R is the universal gas constant (8.314 J mol^{-1} K^{-1}), T is temperature while K stands for the distribution coefficient for the solid-liquid system defined as a ratio of oil concentrations in liquid and solid phase at saturation:

$$K = \frac{C_{oil}^{\text{liquid-phase}}}{C_{oil}^{\text{liquid-phase}}} = \frac{Y_\infty}{Y_0 - Y_\infty} \tag{9}$$

where Y_0 is the amount of oils in the solid at the beginning of the extraction (determined by the Soxhlet extraction) and Y_∞ is oil yield at saturation.

The K values at each temperature were calculated according to equation (9). Diagrams representing values of ln$K$ as a function of reciprocal temperature were plotted for each particle size. ΔH^0 and ΔS^0 were obtained by linear regression.

The Gibbs free energy change (ΔG^0) was calculated according to Eq. (10):

$$\Delta G^0 = \Delta H^0 - T \bullet \Delta S^0 \tag{10}$$

where ΔH^0 and ΔS^0 are changes in enthalpy and entropy, respectively.

2.5.5. Temperature extraction coefficient

Temperature coefficient (γ) as a measure of the increase of oil extraction for every 10 °C was calculated according to Eq. (11):

$$Y_T = Y_{T_0} \bullet \gamma^{\frac{T}{10}} \tag{11}$$

where Y_T and Y_{T_0} are the extraction oil yields at saturation at temperatures T and T_0, respectively.

Temperature coefficient (γ) was calculated by the linearisation of equation (11).

3. Results and discussion

3.1. Extraction of antioxidants

Fig. 2 presents the extraction yields, total phenolic contents and condensed tannins contents for different extraction solvents. The extraction yield was at the highest level when pure ethanol was used as an extraction solvent (9.71%). A similar value of extraction yield (9.33%) was observed for pure methanol, while pure acetone, water, aqueous methanol and ethanol achieved yields ranging from 3.14% to 4.51%. It is interesting to note the influence of relative solvent polarity (acetone 0.36, ethanol 0.65, methanol 0.76 and water 1.00 [27]) on the extraction yield (Fig. 2a)) – a significant increase in the extraction yield was observed when the polarity increased from acetone to ethanol, but the use of solvents with higher polarities (methanol and water) led to a

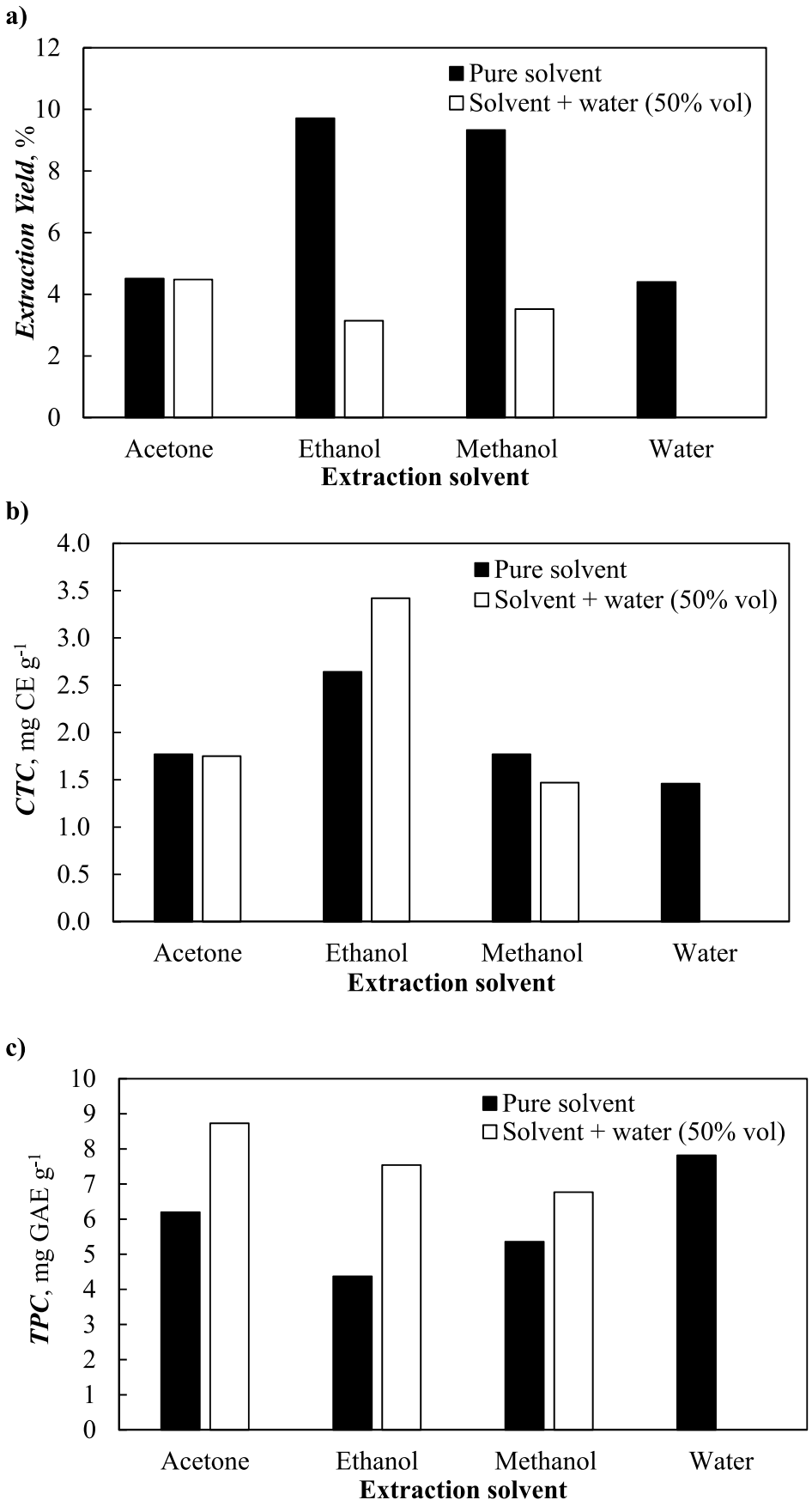

Fig. 2. Extraction yield (a), condensed tannins content (*CTC*) (b), and total phenolic content (*TPC*) (c) of extracts obtained from olive stones using different pure solvents (black bars) and aqueous solvents (white bars). Extraction conditions: temperature 25 °C, extraction time 3 h, solvent-to-solid ratio 20 mL g^{-1}.

reduction in the yield. A similar trend was observed for the condensed tannin content (Fig. 2b)) for both pure and aqueous solvents. On the contrary, extracts obtained with pure solvents gave the lowest total phenolic content for ethanol which was enhanced by a further increase in the solvent polarity (Fig. 2c)).

These trends in *TPC* and *CTC* contents in obtained extracts cannot be explained solely by solvent polarities. The extraction is governed by a complex interplay of various solubilization, transfer and diffusion phenomena. Moreover, both *TPC* and *CTC* present mixtures containing various components with different chemical structures, stereochemistry and the intermolecular forces that occur between them and the solvents.

Antioxidant activities, scavenging activity (*DPPH*) and ferric reducing antioxidant power (*FRAP*) of the extracts obtained from olive stones using different solvents are shown in Fig. 3. The obtained value of 5.36 mgGAE g^{-1} for the extraction from olive stones with pure methanol is comparable with the literature data [28] that range from 1.23 to 7.61 mgGAE g^{-1}. Adding water to pure solvents increased the total phenolic content, but its influence on the extraction yield and condensed tannins content is not straightforward.

The obtained *TPC* in olive stones ranged from 4.37 to 8.73 mgGAE per gram of dry olive stones corresponding to 45 to 240 mgGAE per gram of dry extract. These *TPC* values are comparable with the *TPC* in olives (5.9 mgGAE g^{-1} (dry olives)) [29], olive leaves extracts (42–190 mgGAE g^{-1} (dry extract)) [30] but lower than in olive pomace (200–240 mg mgGAE g^{-1} (dry pomace)) [31].

Data points used in Figs. 2 and 3 are included in Table S2 (supplementary information).

The results of in vitro antioxidant activity assays carried out to assess the capacity of olive stone extracts to scavenge the 2,2-di (4-tert-octylphenyl)-1-picrylhydrazyl radical (DPPH·), as well as their ability to reduce ferric (III) iron to ferrous (II) iron, are presented in Fig. 3. A lower value of IC50 indicates a higher antioxidant activity. It can be observed

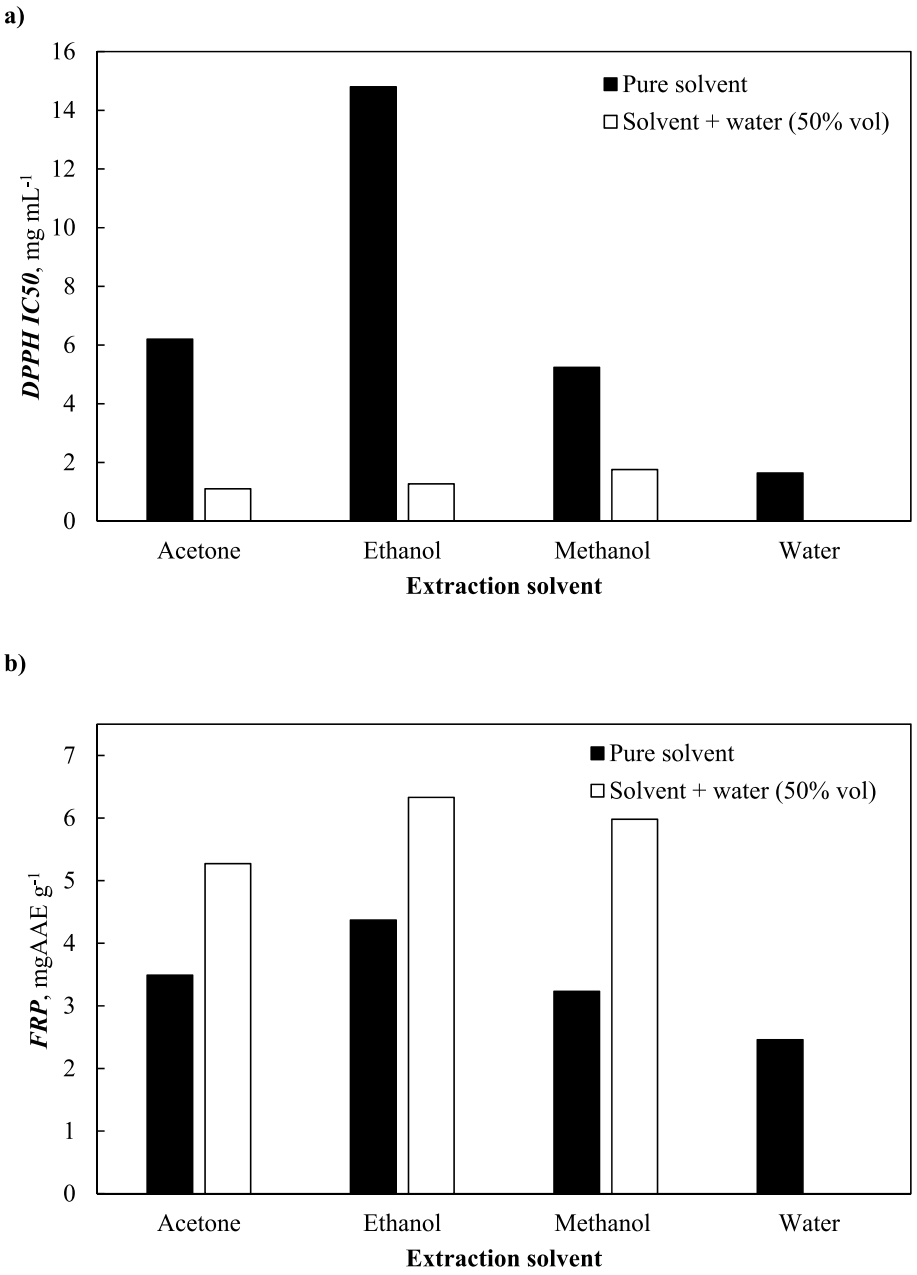

Fig. 3. Antioxidant activities – scavenging activity (*DPPH*) and ferric reducing antioxidant power (*FRAP*) of the extracts obtained from olive stones using different pure solvents (black bars) and aqueous solvents (white bars). Extraction conditions: temperature 25 °C, extraction time 3 h, solvent-to-solid ratio 20 mL g^{-1}.

from Fig. 3a) that the aqueous solutions of acetone and ethanol exhibited the best DPPH scavenging capacity, followed by aqueous methanol and pure water. Significantly weaker DPPH scavenging capacities were observed for pure acetone, ethanol and methanol with IC50 values of 6.20, 14.80 and 5.24 mg mL^{-1}, respectively. These IC50 values indicate somewhat lower antioxidant activities of olive stones extracts compared with extracts obtained from olive leaves (0.02–0.095 mg mL^{-1}) [30] and other waste agricultural products, such as orange peel (0.8–1.4 mg mL^{-1}) [32], banana peel (lower than 0.15 mg mL^{-1}) [33], banana rachis (3.915 mg mL^{-1}) [34] and essential oils from *Abrus precatorius* (1.20–2.10 mg mL^{-1}) [35]. Reducing power as a measure of the conversion of a Fe^{3+} ferricyanide complex to the ferrous form showed that all extracts have a modest ferric reducing power ranging from 2.46 to 6.33 mg AAE g^{-1}. Using aqueous organic solvents resulted in a significant enhancement of the *FRAP* values.

Regression analysis was employed to reveal the relationship between the antioxidant activity (*DPPH* and *FRAP*) and the phenolic composition (*TPC* and *CTC*) of the studied extracts. Strong relationships were observed between antioxidant capacity *DPPH* (reciprocal IC50) and *TPC* ($r^2 = 0.8711$, p-value = 0.002) but not between *DPPH* (reciprocal IC50) and *CTC* ($r^2 = 0.5590$, p-value = 0.252). No correlation of *FRAP* was found with either *TPC* or *CTC*. However, a better correlation was obtained if considering only pure solvent and excluding aqueous organic solvents, resulting in the following values for the relationship between *FRAP* and *TPC* ($r^2 = 0.9178$, p-value = 0.082) and between *FRAP* and CDC ($r^2 = 0.9052$, p-value = 0.049). This analysis demonstrated that the antioxidant potential depended on both the concentrations and the structures of phenolic compounds, which agrees with trends observed by Yu et al. [36].

Once extracts are consumed and go through the digestive system, their antioxidant activity is affected by surrounding pH, temperature, oxygen content, light intensity, enzyme activity, solubility, and interaction with other dietary ingredients. Therefore, studying how gastric and intestinal environments affect antioxidant activity is important as these can diminish health benefits. To this end, the extract obtained by aqueous ethanol exhibited the highest antioxidant activity (highest *FRAP* and low *DPPH* values) and was selected for a simulated digestion procedure. Fig. 4 shows that the total phenolic content is significantly affected by gastric digestion, decreasing from 7.52 to 1.31 mg GAE g^{-1} followed by a further decline to 0.57 mg GAE g^{-1} when extracts are exposed to intestinal digestion. A less significant decrease was observed for condensed tannins content, from 3.42 to 2.66 mg CE g^{-1}. The loss of phytochemicals reflected the antioxidant capacity after digestion: DPPH IC50 value increased three times and *FRAP* decreased almost five times with respect to the values obtained for original extracts. These results show that polyphenols are sensitive to conditions found in gastrointestinal digestion, causing the degradation and significant loss of antioxidant activity, as previously demonstrated for various plant extracts rich in polyphenols [37].

3.2. Extraction of oils

Soxhlet hexane extraction from olive stones resulted in an oil yield of 10.8%, which agrees with the previously reported yields of 5.9–9.8% using Soxhlet hexane extraction for 8 h [38]. Kinetics of the oil extraction from olive stones using n-hexane at various temperatures is given in Fig. 5 for two particle sizes, 1.04 mm (Fig. 5a)) and 3.10 mm (Fig. 5b)). The associated data are presented in Table S3 (Supplementary Info). In the beginning, the extraction was fast, controlled by washing, by which n-hexane rapidly solubilizes the oil available on the surface of olive stone particles. Afterwards, the extraction rate reduced significantly, as the process is controlled by oil diffusion from solid to surface. The extraction rates in both stages were enhanced by increasing temperatures – the highest obtained yield was 9.8% when using particle sizes of 1.04 mm at 60 °C. Higher oil yields and faster kinetics were achieved at a constant temperature for smaller particle sizes due to greater surface area for mass transfer.

Experimental data were fitted by the phenomenological model (Eq. (3)). Obtained parameters, f, k_w and k_d are presented in Table 1. The experimental data and calculated results were in good agreement, demonstrated by the root mean square deviation (*RMSD*), which varied from 0.1028 to 0.4555 and coefficient of determination (r^2) which varied from 0.9647 to 0.9947. The fraction of washable oil, f, was almost independent of temperature but was influenced by particle size, similar to the previous report [21]. As reported by Kostic et al. [21] and So et al. [22], the temperature increase enhanced both mass transfer coefficients for washing and diffusion. The mass transfer coefficient for washing was slightly higher for larger particles at 20 and 30 °C, but similar values

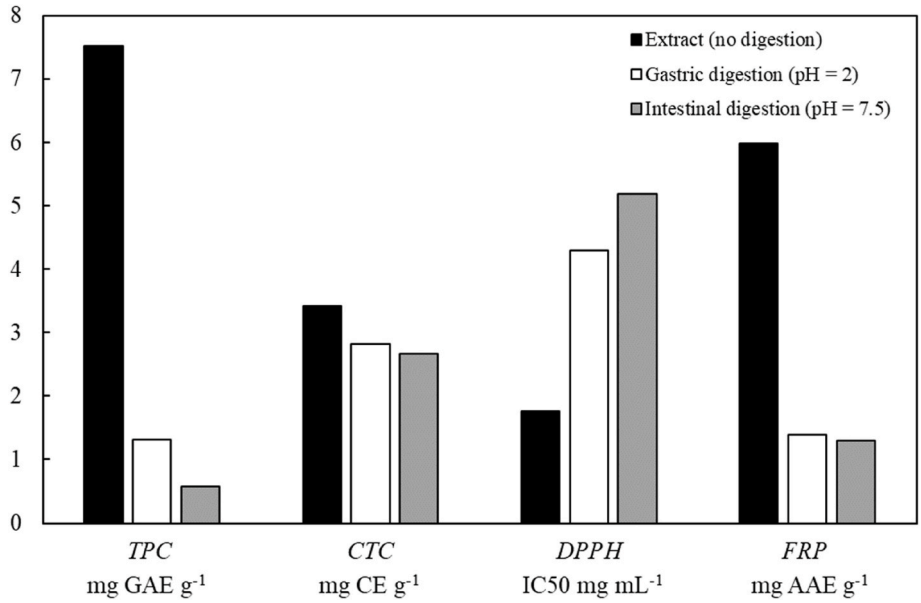

Fig. 4. Effect of gastric and intestinal digestion on total phenolic content (*TPC* in mgGAE g^{-1}), condensed tannin content (*CTC* in mgCE g^{-1}) and antioxidant activities – free radical-scavenging activity (*DPPH* in IC50 mg mL^{-1}) and ferric reducing antioxidant power (*FRAP* in mgAAE g^{-1})). Extraction conditions: solvent ethanol and water mixture (50% vol), temperature 25 °C, extraction time 3 h, solvent-to-solid ratio 20 mL g^{-1}.

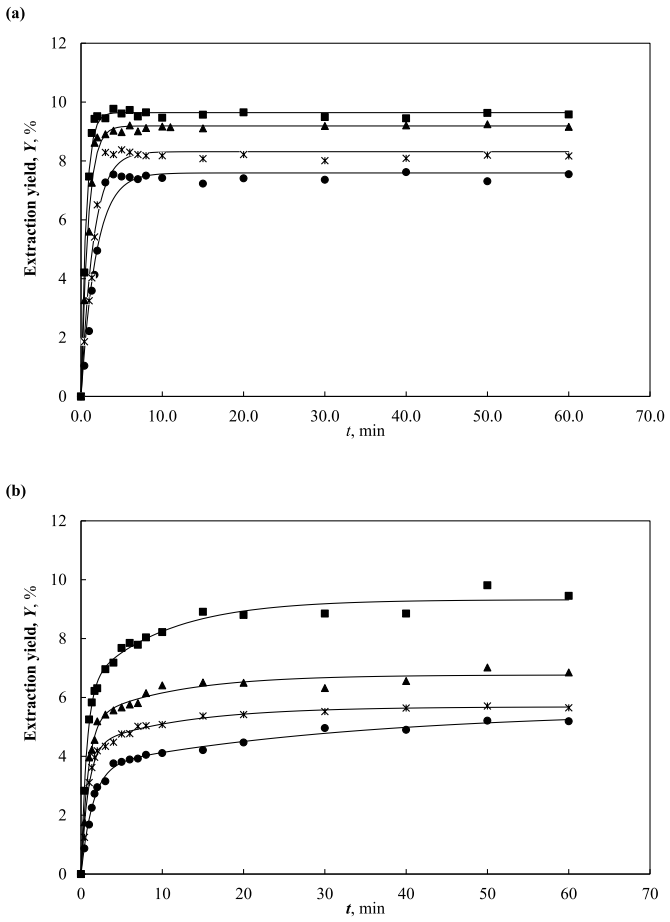

Fig. 5. Oil extraction yield using n-hexane as extraction solvent over time at different temperatures, 20 °C (circles), 30 °C (asterisks), 50 °C (triangles) and 60 °C (squares), using olive stones with a particle size of 1.04 mm (a), and 3.10 mm (b). The solvent-to-solid ratio was 15 mL g^{-1}. Solid lines correspond to the phenomenological model, equation [3]. (For interpretation of the references to colour in this figure legend, the reader is referred to the Web version of this article.)

were observed at 50 and 60 °C. On the contrary, the mass transfer coefficient for diffusion is approximately one order of magnitude higher for smaller particles. It is also worth noting that the values of k_w and k_d are identical for smaller particles at a given temperature, indicating that the extraction process is controlled by both washing and diffusion mechanisms. On average, k_w is 15 times higher than k_d for larger particles indicating a diffusion-controlled extraction process.

The dominant controlling mechanism was identified by comparing ECM and DCM against the experimental data at three temperatures (20 °C, 50 °C, 60 °C) for two different particle sizes. The tuning parameter was τ, to search for the best possible fit to the experimental results.

Fig. 6 shows the ECM and DCM predictions against experimental data at different temperatures for particles of 1.04 mm diameter. Even though both models possess nonlinear trends and perform similarly in predicting the overall time of the extraction process, the ECM presents a better fit to experimental data. The process trajectory is well predicted by ECM, demonstrating that, for 1.04 mm particles, the extraction rate is the dominant controlling mechanism in the investigated temperature range (20 °C–60 °C).

The ECM performance can be explained based on the small size of the particle and, therefore, the thinner ash layer that may form. This is in agreement with Fick's law, which states that the diffusion rate is inversely proportional to the thickness of the diffusion medium. The DCM performance at an early stage of the process supports this conclusion. The DCM model deviation from reality is more significant at lower yield values (beginning of the process). Over this stage, the ash layer is very thin and the extraction rate mainly follows the intrinsic rate expression. With extraction progress, the ash layer thickness and hence the diffusion barrier increase.

Fig. 7 compares the ECM and DCM results against experimental data at different temperatures for particles of 3.1 mm diameter. For this particle size, the DCM presents a greater fit to the experimental data in contrast to the ECM. The ECM performs poorly in predicting both process history and completion time. For particles of 3.1 mm size, the extraction rate is dominated by diffusion as the main controlling mechanism in the investigated temperature range (20 °C–60 °C). The diffusion becomes very slow at a yield of about 0.8 and, beyond that, causes a serious barrier for the whole extraction process. This observation further shows the role of extracted layer mass transfer resistance. This has been observed at all temperatures, even though the maximum yield is achieved in a shorter time at a higher temperature.

The thermodynamic analysis was conducted to calculate enthalpy change (ΔH^0), entropy change (ΔS^0) and Gibbs free energy change (ΔG^0) of the oil extraction process. The distribution coefficient (K) values at different extraction temperatures were calculated using Eq. (9) and shown in Table 2. The increase in temperature enhanced K due to the change in solid-liquid equilibria. Extraction involving smaller particles showed higher values of partition coefficients for all studied temperatures because the concentration of oil in a solvent at saturation is higher.

Fig. 8 shows the linear relationship of ln K and reciprocal temperature for two different particle sizes. The ΔH^0 and ΔS^0 were obtained from the slope and intercept of the straight lines according to Eq. (8). Subsequently, ΔG^0 was calculated using Eq. (10). All thermodynamic values are presented in Table 2. Obtained values for ΔH^0 for the oil extraction from olive stones were positive for both particle sizes, indicating that 25.29 and 26.16 kJ mol^{-1} of energy should be absorbed to enable the extraction process, respectively. These values are higher than the reported 6.17–10.54 kJ mol^{-1} [21], 11.2 kJ mol^{-1} [39], 12.9 kJ mol^{-1} [40], for extraction of oils from hemp seeds, sunflower seeds and olive cake, respectively; but much lower than those for soybean flakes (48.2–95.4 kJ mol^{-1}) [41] and cottonseeds (43.2–85.8 kJ mol^{-1}) [42]. The calculated values for ΔS^0 (92.72 and 86.64 J mol^{-1}) are positive,

Table 1
Parameters of the phenomenological model (Eq. [3]) for oil extraction from olive stones using n-hexane as a solvent (15 mL g^{-1}).

Particle diameter	T	$Y_{\infty,exp}$	$Y_{\infty,calc}$	f	k_w	k_d	r^2	$RMSD$
	°C	%	%	–	min^{-1}	min^{-1}	–	–
1.04 mm	20	7.59	7.41	0.092	0.541	0.541	0.9647	0.4555
	30	8.31	8.14	0.092	0.656	0.656	0.9710	0.4248
	50	9.19	9.18	0.102	1.160	1.160	0.9864	0.2806
	60	9.64	9.55	0.108	1.597	1.597	0.9915	0.2208
3.10 mm	20	5.57	4.72	0.652	0.689	0.030	0.9947	0.1028
	30	5.68	5.48	0.758	1.125	0.085	0.9926	0.1267
	50	6.76	6.60	0.769	1.159	0.094	0.9896	0.1778
	60	9.32	8.98	0.678	1.423	0.102	0.9923	0.2051

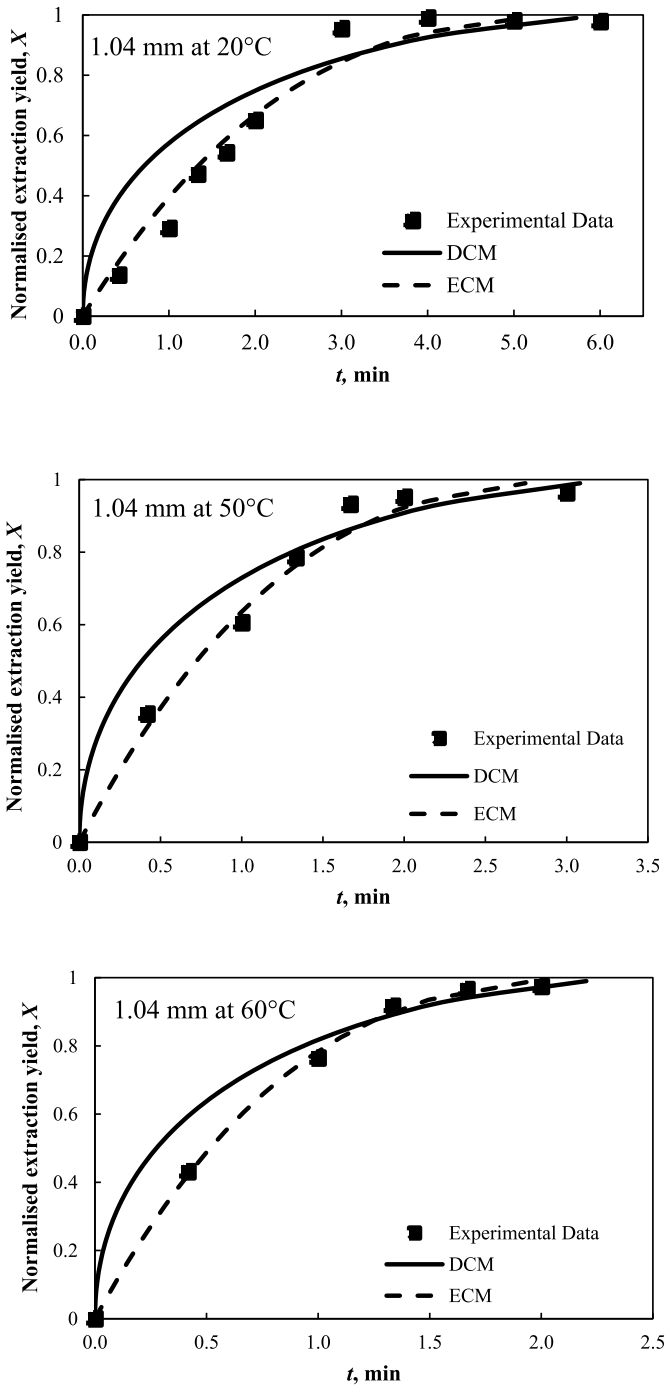

Fig. 6. Comparison of the extraction-control model (ECM) and diffusion-control model (DCM) predictions against experimental data at different temperatures for particles of 1.04 mm diameter.

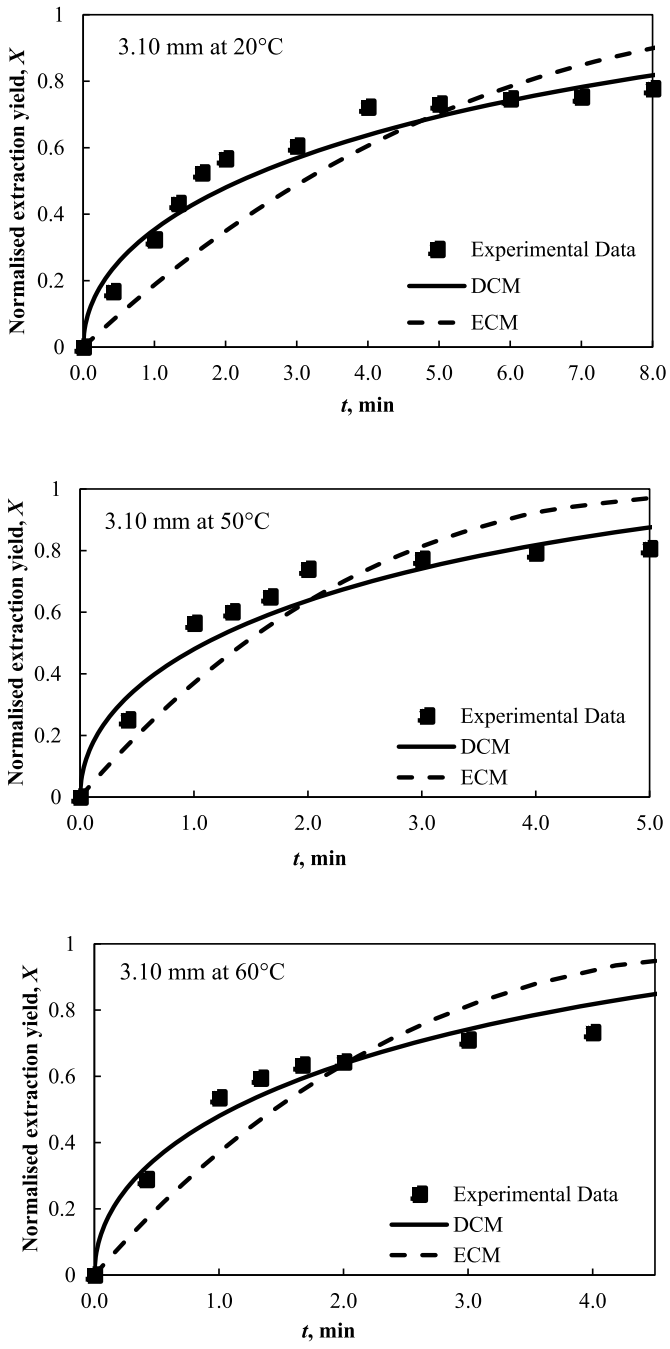

Fig. 7. Comparison of the extraction-control model (ECM) and diffusion-control model (DCM) predictions against experimental data at different temperatures for particles of 3.10 mm diameter.

indicating an irreversible process which is well within the reported values in the aforementioned literature. The Gibbs free energy change was negative for all conditions except for oil extraction from olive stones of 3.10 mm particle size at 20 °C. The negative ΔG^0 values mean that the process is feasible and spontaneous. Increasing the temperature and decreasing the particle size enhanced the spontaneity of the oil extraction suggested by more negative values of ΔG^0.

Temperature coefficients (γ), demonstrating a factor of the oil yield increase for every 10 °C rise in temperature, were calculated by the linearisation of Eq. (11). The obtained values were 1.06 and 1.15 for olive stones with an average particle size of 1.04 mm and 3.10 mm, respectively. These values indicate the factor of oil yield increase for every 10 °C in the experimental temperature range (20–60 °C). These values are similar to the previously reported for the oil extraction from olive cake (1.02–1.14) [40] and hempseeds (1.01–1.03) [21].

4. Conclusions

This paper shows that extraction from olive stones using various solvents affects the yield, polyphenol content and tannins content, and antioxidant activity. The extracts obtained by aqueous ethanol solvent (50% vol) exhibited the highest antioxidant activity with the *DPPH* IC50 of 1.27 mg mL^{-1} and ferric reducing antioxidant power (*FRAP*) of 6.33 mgAAE g^{-1}. These results are comparable with the antioxidant activities

Table 2
Partition coefficient (K) and thermodynamic quantities (enthalpy change, entropy change and Gibbs free energy change) for oil extraction from olive stones using n-hexane.

Particle size	T	K	ΔS	ΔH	ΔG	r^2
	°C	–	J mol^{-1} K^{-1}	kJ mol^{-1}	kJ mol^{-1}	–
1.04 mm	20	2.19	92.72	25.29	−1.90	0.9998
	30	3.05			−2.82	
	50	5.65			−4.68	
	60	7.63			−5.60	
3.10 mm	20	0.78	86.64	26.16	0.76	0.9189
	30	1.03			−0.11	
	50	1.57			−1.84	
	60	3.19			−2.71	

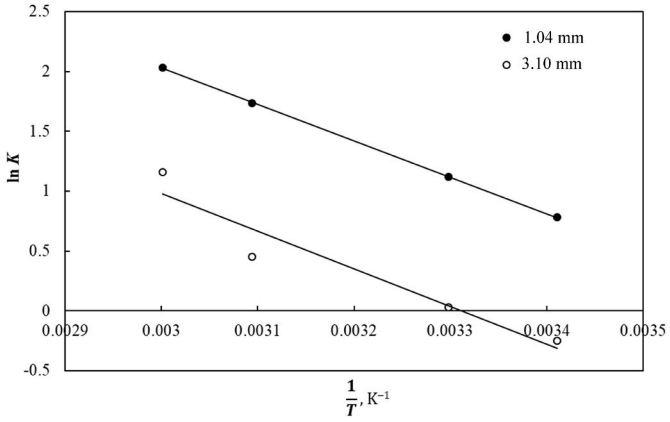

Fig. 8. Dependence of ln$K$ on reciprocal temperature for two olive stone particle sizes: 1.04 mm (blacked circles) and 3.10 mm (white circles).

of commercially available supplements from other agricultural waste products, indicating the potential to use olive stones as a source.

After in vitro digestion composed of gastric and intestinal processes, the antioxidant activity of olive stones decreased: *DPPH* IC50 value increased three times and *FRAP* decreased almost five times with respect to the values obtained for original extracts.

This paper reports the kinetics of oil extractions from olive stones for the first time, which is of twofold importance: 1) removal of oils from olive stones is essential pre-treatment to decrease emissions of hazardous gases and particulate matter in the combustion process, making olive stones more sustainable biofuel; and, 2) extracted oils can be used as a raw material for biodiesel production. Both phenomenological and shrinking core models (SCM) were used to fit these kinetics data and showed good agreement with experimental data. Both models showed that diffusion and intrinsic extraction rate are dominant mechanisms while the particle size strongly influences their contributions. The presented SMC model can be further advanced to generate a reactor scale model that considers mass and heat transfers as well as hydrodynamics of the bulk solvent, which is essential for scale-up and systems integration purposes.

The thermodynamic analysis showed that the extraction process is endothermic, irreversible and spontaneous under most studied conditions. Increasing the temperature and decreasing the particle size enhanced the spontaneity of the oil extraction suggested by more negative values of ΔG^0. The temperature coefficients were 1.06 and 1.15 for smaller and larger olive stone particles, respectively.

Data reported in this work can be used to design the valorization process to obtain extracts rich in antioxidants, oils and more sustainable biofuel from waste olive stones, which can generate additional revenues for the agricultural waste industry while enhancing sustainability and resilience to market volatility. This can particularly benefit the economic sector in many rural areas of the Mediterranean and northern parts of Africa, which are the biggest producers of olive oil.

Data availability

All data are included in the manuscript.

Acknowledgements

This work was supported by the Engineering and Physical Sciences Research Council – Impact Acceleration Account.

Appendix A. Supplementary data

Supplementary data to this article can be found online at https://doi.org/10.1016/j.biombioe.2022.106623.

References

[1] C.S.K. Lin, L.A. Pfaltzgraff, L. Herrero-Davila, E.B. Mubofu, S. Abderrahim, J. H. Clark, A.A. Koutinas, N. Kopsahelis, K. Stamatelatou, F. Dickson, S. Thankappan, Z. Mohamed, R. Brocklesbyc, R. Luque, Food waste as a valuable resource for the production of chemicals, materials and fuels. Current situation and global perspective, Energy Environ. Sci. 6 (2013) 426–464.
[2] C.F. Fava, G. Totaro, L. Diels, M. Reis, J. Duarte, O.B. Carioca, H.M. Poggi-Varaldo, B.S. Ferreira, Biowaste biorefinery in Europe: opportunities and research & development needs, N. Biotech. 32 (2015) 100–108.
[3] J.F. García Martín, M. Cuevas, C. Feng, P.A. Mateos, M.T. García, S. Sánchez, Energetic valorisation of olive biomass: olive-tree pruning, olive stones and pomaces, Processes 8 (2020) 511.
[4] C. Pattara, G.M. Cappelletti, A. Cichelli, Recovery and use of olive stones: commodity, environmental and economic assessment, Renew. Sustain. Energy Rev. 14 (2010) 1484–1489.
[5] I. Mediavilla, R. Barro, E. Borjabad, D. Peña, M.J. Fernández, Quality of olive stone as a fuel: influence of oil content on combustion process, Renew. Energy 160 (2020) 374–384.
[6] S. Chanioti, C. Tzia, Processing parameters on the extraction of olive pomace oiland its bioactive compounds: a kinetic and thermodynamic study, J. Am. Oil Chem. Soc. 95 (2018) 371–382.
[7] G. Rodríguez, A. Lama, R. Rodríguez, A. Jiménez, R. Guillén, J. Fernández-Bolaños, Olive stone an attractive source of bioactive and valuable compounds, Bioresour. Technol. 99 (2008) 5261–5269.
[8] D. Ryan, P.D. Prenzler, S. Lavee, M. Antolovich, K. Robards, Quantitative changes in phenolic content during physiological development of the olive (olea europaea) cultivar Hardy's mammoth, J. Agric. Food Chem. 51 (2003) 2532–2538.
[9] A. Karković Marković, J. Torić, M. Barbarić, C. Jakobušić Brala, Hydroxytyrosol, tyrosol and derivatives and their potential effects on human health, Molecules 24 (2019) 2001.
[10] A. Lama-Muñoz, J.M. Romero-García, C. Cara, M. Moya, E. Castro, Low energy-demanding recovery of antioxidants and sugars from olive stones as preliminary steps in the biorefinery context, Ind. Crop. Prod. 60 (2014) 30–38.
[11] U.G. Spizzirri, D. Restuccia, S. Chiricosta, O.I. Parisi, G. Cirillo, M. Curcio, F. Iemma, F. Puoci, N. Picci, J. Food and Nutr. Res. 50 (2011) 57–67.
[12] J. Bouayed, L. Hoffmann, T. Bohn, Total phenolics, flavonoids, anthocyanins and antioxidant activity following simulated gastro-intestinal digestion and dialysis of apple varieties: bioaccessibility and potential uptake, Food Chem. 128 (2011) 14–21.
[13] K. Wojtunik-Kulesza, A. Oniszczuk, T. Oniszczuk 2, M. Combrzynski, D. Nowakowska, A. Matwijczuk, Influence of in vitro digestion on composition, bioaccessibility and antioxidant activity of food polyphenols—a non-systematic review, Nutrients 12 (2020) 1401.
[14] A. Alegría, G. Garcia-Llatas, A. Cilla, Static digestion models: general introduction, et-al, in: The Impact of Food Bioactives on Health, Springer, Cham, 2015.
[15] M.P. Kähkönen, A.I. Hopia, H.J. Vuorela, J.-P. Rauha, K. Pihlaja, T.S. Kujala, M. Heinonen, Antioxidant activity of plant extracts containing phenolic compounds, J. Agric. Food Chem. 47 (1999) 3954–3962.
[16] T. Swain, W.E. Hillis, The phenolics constituents of prunus domestica. I. The quantitative analysis of phenolics constituents, J. Sci. Food Agric. 10 (1959) 63–68.
[17] G. Kroyer, N. Hegedus, Evaluation of bioactive properties of pollen extracts as functional dietary food supplement, Innovat. Food Sci. Emerg. Technol. 2 (2001) 171–174.
[18] A. Yıldırım, M. Oktay, V. Bilalõglu, The antioxidant activity of the leaves of Cydonia vulgaris, Turk. J. Med. Sci. 31 (2001) 23–27.
[19] M.-J. Bermúdez-Soto, F.-A. Tomás-Barberán, M.-T. García-Conesa, Stability of polyphenols in chokeberry (Aronia melanocarpa) subjected to in vitro gastric and pancreatic digestion, Food Chem. 102 (2007) 865–874.
[20] J. Boyer, D. Brown, R.H. Liu, In vitro digestion and lactase treatment influence uptake of quercetin and quercetin glucoside by the Caco-2 cell monolayer, Nutr. J. 4 (2005) 1.

[21] M.D. Kostić, N.M. Joković, O.S. Stamenković, K.M. Rajković, P.S. Milić, V. B. Veljković, The kinetics and thermodynamics of hempseed oil extraction by n-hexane, Ind. Crop. Prod. 52 (2014) 679–686.
[22] G.C. So, D.G. Macdonald, Kinetics of oil extraction from canola (rapeseed), Can. J. Chem. Eng. 64 (1986) 80–86.
[23] S. Yagi, D. Kunii, Studies on combustion of carbon particles in flames and fluidized beds, Symposium (International) on Combustion 5 (1) (1955) 231–244.
[24] S. Yagi, D. Kunii, Fluidized-solids reactors with continuous solids feedi: residence time of particles in fluidized beds, Chem. Eng. Sci. 16 (1961) 364–371.
[25] A. Amiri, G.D. Ingram, N.E. Maynard, I. Livk, A.V. Bekker, An unreacted shrinking core model for calcination and similar solid-to-gas reactions, Chem. Eng. Commun. 202 (2015) 1161–1175.
[26] A. 2Amiri, G.D. Ingram, A.V. Bekker, I. Livk, N.E. Maynard, A multi-stage, multi-reaction shrinking core model for self-inhibiting gas-solid reactions, Adv. Powder Technol. 24 (4) (2013) 728–736.
[27] C. Reichardt, Solvents and Solvent Effects in Organic Chemistry, third ed., Wiley-VCH Publishers, 2003.
[28] H. Hannachi, W. Elfalleh, M. Laajel, I. Ennajeh, R.F. Mechlouch, K. Nagaz, Chemical profiles and antioxidant activities of leaf, pulp, and stone of cultivated and wild olive trees (OleaEuropaea L.), Int. J. Fruit Sci. 20 (2020) 350–370.
[29] S. McDonald, P.D. Prenzler, M. Antolovich, K. Robards, Phenolic content and antioxidant activity of olive extracts, Food Chem. 73 (2001) 73–84.
[30] S. Ghasemi, D.E. Koohi, M.S.B. Emmamzadehhashemi, S.S. Khamas, M. Moazen, A. K. Hashemi, G. Amin, F. Golfakhrabadi, Z. Yousefi, F. Yousefbeyk, Investigation of phenolic compounds and antioxidant activity of leaves extracts from seventeen cultivars of Iranian olive (Olea europaea L.), J. Food Sci. Technol. 55 (2018) 4600–4607.
[31] L. Lesage-Meessen, D. Navarro, S. Maunier, J.-C. Sigoillot, J. Lorquin, M. Delattre, J.-L. Simon, M. Asther, M. Labat, Simple phenolic content in olive oil residues as a function of extraction systems, Food Chem. 75 (2001) 501–507.
[32] J.-H. Park, M. Lee, E. Park, Antioxidant activity of orange flesh and peel extracted with various solvents, Prev. Nutr. Food Sci. 19 (2014) 291–298.
[33] I. Fidrianny, N.A.S. Anggraeni, M. Insanu, Antioxidant properties of peels extracts from three varieties of banana (Musa sp.) grown in West Java-Indonesia, Int. Food Res. J. 25 (2018) 57–64.
[34] S. Díaz, A.N. Benítez, S. Ramírez-Bolaños, L. Robaina, Z. Ortega, Optimization of Banana Crop By-Products Solvent Extraction for the Production of Bioactive Compounds, Biomass Conv. Bioref., 2021.
[35] S.O. Okoh, O.T. Asekun, O.B. Familoni, A.J. Afolayan, Antioxidant and free radical scavenging capacity of seed and shell essential oils extracted from Abrus precatorius (L), Antioxidants 3 (2014) 278–287.
[36] M. Yu, I. Gouvinhas, J. Rocha, A.I.R.N. A Barros, Phytochemical and antioxidant analysis of medicinal and food plants towards bioactive food and pharmaceutical resources, Sci. Rep. 11 (2021), 10041.
[37] M.-J. Bermúdez-Soto, F.-A. Tomás-Barberán, M.-T. García-Conesa, Stability of polyphenols in chokeberry (Aronia melanocarpa) subjected to in vitro gastric and pancreatic digestion, Food Chem. 102 (2007) 865–874.
[38] G. Moghaddam, Y. Vander Heyden, Z. Rabiei, N. Sadeghi, M.R. Oveisi, B. Jannat, V. Araghi, S. Hassani, M. Behzad, M. Hajimahmoodi, Characterization of different olive pulp and kernel oils, J. Food Compos. Anal. 28 (2012) 54–60.
[39] H. Topallar, U. Gecgel, Kinetics and thermodynamics of oil extraction from sunflower seeds in the presence of aqueous acidic hexane solutions, Turk. J. Chem. 24 (2000) 247–253.
[40] S. Meziane, H. Kadi, Kinetics and thermodynamics of oil extraction from olive cake, J. Am. Oil Chem. Soc. 85 (2008) 391–396.
[41] C.E.C. Rodrigues, K.K. Aracava, F.N. Abreu, Thermodynamic and statistical analysis of soybean oil extraction process using renewable solvent, Food Sci. Technol. Int. 45 (2010) 2407–2414.
[42] D.K. Saxena, S.K. Sharma, S.S. Sambi, Kinetics and thermodynamics of cottonseed oil extraction, Grasas Aceites 62 (2011) 198–205.